J. Cell. Mol. Med. Vol 16, No 8, 2012 pp. 1916–1923

Altered apoptosis regulation in Kufor–Rakeb syndrome patients with mutations in the *ATP13A2* gene

Elena Radi, Patrizia Formichi, Giuseppe Di Maio, Carla Battisti, Antonio Federico*

Department of Neurological, Neurosurgical and Behavioural Sciences, University of Siena, Siena, Italy

Received: May 19, 2011; Accepted: November 17, 2011

Abstract

ATP13A2 gene encodes for a protein of the group 5 P-type ATPase family. *ATP13A2* mutations are responsible for Kufor–Rakeb syndrome (KRS), a rare autosomal recessive juvenile parkinsonism characterized by the subacute onset of extrapyramidal, pyramidal and cognitive dysfunction with secondary nonresponsiveness to levodopa. FBXO7 protein is an F-box-containing protein. Recessive *FBXO7* mutations are responsible for PARK15, a rare juvenile parkinsonism characterized by progressive neurodegeneration with extrapyramidal and pyramidal system involvement. Our aim was to evaluate apoptosis in cells from two KRS siblings carrying a homozygous *ATP13A2* mutation and a heterozygous *FBXO7* mutation. We also analysed apoptosis in the patients' healthy parents. Peripheral blood lymphocytes from the KRS patients and parents were exposed to 2-deoxy-D-ribose; apoptosis was analysed by flow cytometry and fluorescence microscopy. Apoptosis was much higher in lymphocytes from the KRS patients and parents than in controls, both in standard conditions and after induction with a pro-apoptotic stimulus. The lack of correlation between increased apoptosis and the presence of the mutated *FBXO7* gene rules out the involvement of *FBXO7* in apoptosis regulation. The altered apoptotic pattern of subjects with mutated *ATP13A2* suggests a correlation between apoptosis alteration and the mutated ATP13A2 protein. We hypothesize that *ATP13A2* mutations may compromise protein function, disrupting cell cation balance and rendering cells prone to apoptosis. However, the deregulation of apoptosis in KRS patients displaying different disease severity suggested that the altered apoptotic pathway probably does not have a pathogenetic role in KRS by itself.

Keywords: Kufor–Rakeb syndrome • apoptosis • caspase 8 • Parkinsonism

Introduction

The *ATP13A2* gene encodes for a large transmembrane protein belonging to the group 5 P-type ATPase family. P-type ATPases are a large superfamily of proteins, present both in prokaryotes and eukaryotes, which are involved in the transport of inorganic cations and other substrates across membranes [1]. *ATP13A2* encodes a 1180 amino acid protein that localizes to the lysosomes [2]. The substrate specificity of ATP13A2 protein remains unknown, although there is evidence that this protein is involved in the transport of cations from the cytosol to the lysosomal lumen [3, 4] and it has been suggested that compromised ATP13A2 function may disrupt the balance of essential divalent cations [4]. Moreover, a recent study has demonstrated that the yeast homologue of human ATP13A2 (Ypk9) can suppress α-synuclein toxicity and protect cells from manganese toxicity [3]. Homozygous and compound heterozygous mutations in *ATP13A2* are responsible for Kufor–Rakeb syndrome (KRS or PARK9), a rare form of autosomal recessive juvenile parkinsonism that was first described in 1994 by Najim al-Din *et al.* [5]. KRS is a levodopa-responsive Parkinsonian disorder characterized by the subacute onset of extrapyramidal, pyramidal and cognitive dysfunction. The disease appears to progress rapidly in the first year and then more insidiously thereafter, with increasing parkinsonism, pyramidal signs, cognitive deterioration and secondary nonresponsiveness to levodopa [6]. The pathology of KRS remains largely unexplored, although neuroimaging has shown progressive, diffuse brain atrophy [7].

The *FBXO7* gene encodes for an F-box protein component of the E3 ubiquitin ligases, SCF complexes (Skp1, Cdc53/Cullin1, F-box protein) [8]. Recessive mutations in the *FBXO7* gene are responsible for a novel additional and rare form of juvenile parkinsonism, known as PARK15 (monogenic parkinsonism

*Correspondence to: Prof. Antonio FEDERICO,
Department of Neurological, Neurosurgical and Behavioural Sciences,
Policlinico "Le Scotte" V.le Bracci 2,
53100 Siena, Italy.
Tel.: +39 0577 585763
Fax: +39 0577 40327
E-mail: federico@unisi.it

doi:10.1111/j.1582-4934.2011.01488.x

Table 1 Clinical and molecular features of the two KRS siblings

Patient	Sex	Age	Genetic pattern	Onset	Phenotypic pattern
BA	M	44	ATP13A2 c.G2629A hom FBXO7 c.C14441T het	8	Severe cognitive decline; gait with bilateral support; dysarthria; hypophonia; pyramidal signs in the lower limbs
BC	M	34	ATP13A2 c.G2629A hom FBXO7 c.C14441T het	7	Mild cognitive deterioration; heel walking; brisk tendon reflexes in the lower limbs

type 15), characterized by progressive neurodegeneration with extrapyramidal and pyramidal system involvement.

In this study we used peripheral blood lymphocytes (PBLs) as a cell model to evaluate the presence of apoptosis in cells with *ATP13A2* mutations. We analysed PBLs from two KRS patients carrying a homozygous *ATP13A2* mutation, who were also characterized by a single heterozygous *FBXO7* mutation. Moreover, we analysed apoptosis in PBLs from the patients' healthy parents, characterized by a heterozygous *ATP13A2* mutation. The probands' mother alone was also characterized by a single heterozygous *FBXO7* mutation. 2-deoxy-D-ribose (dRib), a highly reducing sugar that determines the depletion of reduced glutathione [9], was used as paradigm pro-apoptotic stimulus, as it has already been validated in several previous studies by our group [10–12].

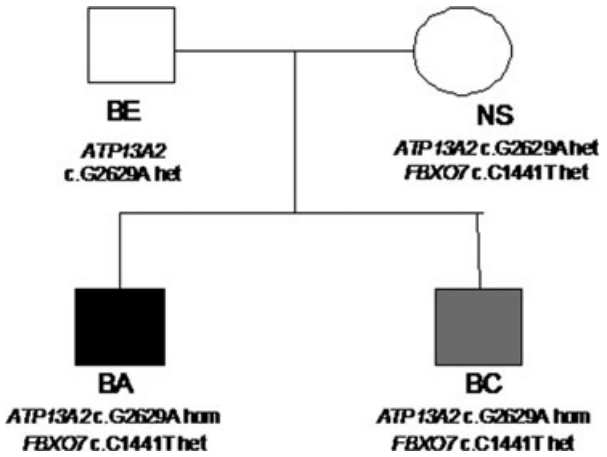

Fig. 1 Simplified pedigree of the KRS family. The patient with the more severe pathology is highlighted by a black symbol, his brother is highlighted in grey.

Materials and methods

Patients

We analysed PBLs from two siblings (BA and BC) with KRS, from their healthy parents (BE and SN) and from four healthy age-matched controls. These KRS patients, previously described by Santoro *et al.* [13], carried the homozygous c.G2629A mutation in exon 24 of the *ATP13A2* gene and the c.C1441T heterozygous mutation in exon 9 of the *FBXO7* gene. Despite their identical genetic pattern, the KRS patients showed significantly different clinical severity. The clinical parameters of the patients are reported in Table 1.

The parents (KRS parents) carried the heterozygous c.G2629A mutation in the *ATP13A2* gene; the mother (SN) also carried the heterozygous c.C1441T mutation in the *FBXO7* gene. A simplified pedigree is shown in Figure 1.

Written consent was obtained from all subjects, and ethical approval was granted by the Local Ethics Committee.

Methods

PBLs from KRS patients and their parents and controls were obtained in an aseptic manner; mononuclear cells were separated by centrifuging on a Lymphoprep gradient [14]. They were washed twice in PBS, resuspended in RPMI 1640 (Sigma-Aldrich, Milan, Italy) supplemented with 10% FCS, 1% L-glutamine, 1% streptomycin–penicillin (Sigma-Aldrich) and sown, at a starting density of 1×10^6 per well, in 6-well plates where they were maintained in a humidified atmosphere with 5% CO2 at 37°C. PBLs were exposed to 10 mM dRib (Sigma-Aldrich) [10]. PBLs were harvested after 1, 24 and 48 hrs of culture and the percentage of apoptotic cells was evaluated by the analysis of DNA content according to the flow cytometric method described by Nicoletti *et al.* [15]. PBLs of KRS patients (BA and BC) and of two controls collected after 1 and 48 hrs of culture were also seeded on microscope slides and analysed for alterations in mitochondrial membrane potential ($\Delta\Psi m$) by JC1 [16], phosphatidylserine (PS) plasma membrane translocation by Annexin V [17], and activation of caspase 3 and 7 by 'FAM-DEVD-FMK Carboxyfluorescein FLICA Apoptosis Detection Kit Caspase Assay' [12], caspase 8 by 'FAM-LETD-FMK Carboxyfluorescein FLICA Apoptosis Detection Kit Caspase Assay' and caspase 9 by 'FAM-LEHD-FMK Carboxyfluorescein FLICA Apoptosis Detection Kit Caspase Assay'. For each patient and control we performed two experiments.

For statistical analysis of citofluorimetric data, KRS patients and parents were collectively analysed as the KRS family, on the basis of the presence, either in homozygous or heterozygous state, of the c.G2629A mutation in exon 24 of the *ATP13A2* gene. Control and KRS family groups were statistically compared by means of the non-parametric two-tailed test of Mann–Whitney. A statistical significance level of 95% ($P < 0.05$) was considered in all cases.

Microscopy analysis was performed using an Axioskop 2 plus microscope (Carl Zeiss Meditec, Inc., Dublin, CA, USA) by two independent observers. For quantitative evaluation of PS externalization and caspase activation, mean percentage ($\pm$S.D.) of positive cells was calculated evaluating five fields for each slide.

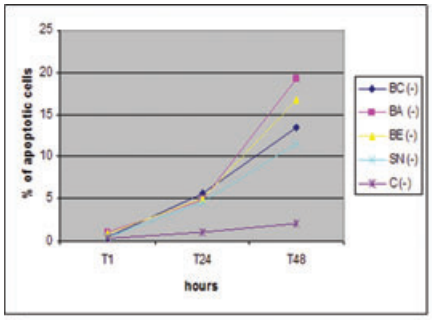

A

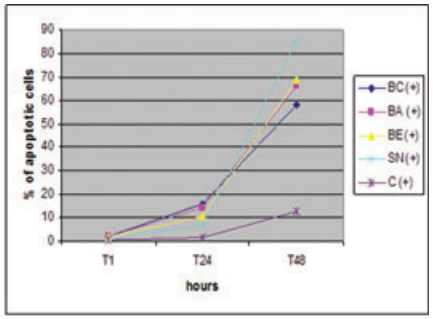

B

C

	T1	T24	T48
BC (-)	0,44	5,65	13,39
BA (-)	1,07	4,88	19,26
BE (-)	0,83	5,01	16,7
SN (-)	0,50	4,54	11,5
BC (+)	2,07	15,73	58,43
BA (+)	2,01	14,05	66,02
BE (+)	1,48	10,52	68,7
SN (+)	1,29	6,84	85,5
C (-)	0,345 (0,09)	1,05 (0,15)	2,13 (0,22)
C (+)	0,365 (0,15)	1,58 (0,23)	12,7 (0,95)

Fig. 2 Cytofluorimetric analysis of apoptotic PBLs from the KRS family (patients: BC and BA; parents: BE and SN) and four controls (C) cultured with (+) or without (–) dRib. Values are expressed as percentages (for controls: median and mad) of apoptotic cells.

Results

Flow cytometry

Flow cytometric analysis showed the DNA content in the sub-G1 region of PBLs from KRS patients, KRS parents and controls, at different times of incubation with or without dRib. PBLs cultured without dRib showed a higher percentage of apoptotic cells in KRS family than in controls and this difference became statistically significant after 24 hrs of culture (Fig. 2A).

After 24 and 48 hrs of culture with dRib the percentage of apoptotic cells in the KRS family and controls was much higher than in untreated cells (Fig. 2B). However, the percentage of apoptotic cells was much higher in PBLs from the KRS family than in those from controls, and the difference between the two groups was already statistically significant after 1 hr of culture ($P < 0.05$). After 48 hrs of incubation with dRib, the percentage of apoptotic PBLs in the KRS family was on average 5.3 ($\pm$0.8) times higher than in controls (Fig. 2C).

Analysis of $\Delta\Psi$m (JC1)

After 1 hr of incubation with dRib, PBLs from controls and KRS patients (BA and BC) showed many brightly stained intact mitochondria (data not shown). After 24 and 48 hrs of culture with dRib, PBLs of both groups showed an increase in fluorescent green mitochondria, reflecting a fall in $\Delta\Psi$m. However, after 48 hrs of culture with dRib, PBLs from KRS patients (Fig. 3A and B) showed more evident green fluorescence than PBLs from controls (Fig. 3C), demonstrating a higher degree of mitochondrial membrane depolarization. PBLs from patients (Fig. 3D and E) also showed a higher degree of mitochondrial depolarization than those of controls (Fig. 3F) even when cultured without dRib (Fig. 3D–F).

Externalization of PS (Annexin V)

We simultaneously analysed PS externalization and cell viability, using AnnV-Cy3 (red fluorescence) and 6-CFDA (green fluorescence), respectively, in PBLs from controls and KRS patients (BA and BC). Mean percentages ($\pm$S.D.) of apoptotic cells at 1 and 48 hrs of incubation are reported in Table 2.

After 1 hr of incubation with and without dRib, PBLs from controls and KRS patients showed the typical pattern of living cells: intense green fluorescence and no red fluorescence (data not shown).

After 48 hrs (Fig. 4A–C) of incubation with dRib, PBLs from both KRS patients (Fig. 4A and B) and controls (Fig. 4C) showed less intense green fluorescence and many red fluorescent cells (double-stained cells were apoptotic); however apoptotic PBLs were more numerous in KRS patients than in controls (Table 2). After 48 hrs of culture without dRib, PBLs from patients (Fig. 4D and E) showed a higher percentage of apoptotic cells than controls (Fig. 4F) (Table 2).

Caspase activation (FLICA)

Mean percentages ($\pm$S.D.) of PBLs showing caspase-3 and -7 activation at 1 and 48 hrs of culture are reported in Table 3. After 1 hr of incubation with and without dRib, PBLs from both controls

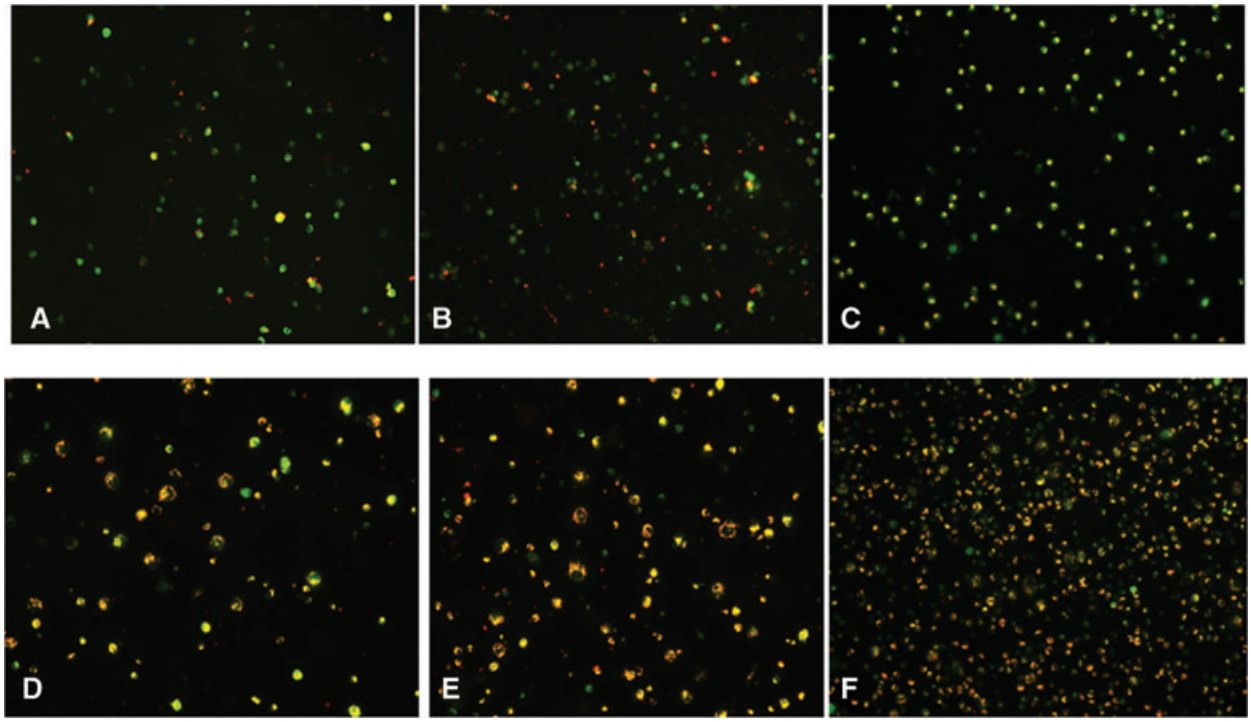

Fig. 3 Evaluation of $\Delta\Psi m$ with JC1 staining in PBLs from KRS patients (BC and BA) and a control representing the group, after 48 hrs of incubation with dRib (**A**–**C**) and after 48 hrs of culture in standard conditions (**D**–**F**). Magnification 20×.

Table 2 Mean percentage (±S.D.) of apoptotic PBLs from KRS patients (BC and BA) and controls (C) evaluated by Annexin V staining

	BC	BA	C
T1–	1.0 ± 0.2	1.5 ± 0.2	0.7 ± 0.4
T48–	12.5 ± 1.4	10.5 ± 1.7	5.6 ± 0.9
T1+	2.1 ± 0.3	2.5 ± 0.7	1.3 ± 0.6
T48+	40.7 ± 3.2	53.9 ± 4.7	7.5 ± 1.9

and KRS patients lacked caspase-3 and -7 activity, as demonstrated by the absence of green fluorescence (data not shown). In both groups a progressive increase in caspase-3 and -7 activity was seen after 48 hrs of incubation with dRib; however the increase was more evident in PBLs from patients (Fig. 5A and B) than in control (Fig. 5C) PBLs (Table 3). After 48 hrs of culture without dRib, PBLs from KRS patients (Fig. 5D and E) showed a higher percentage of caspase-3 and -7 activation than controls (Fig. 5F) (Table 3).

Mean percentages (±S.D.) of PBLs showing caspase-8 activation at 1 and 48 hrs of culture are reported in Table 4. After 1 hr of incubation with and without dRib, PBLs from both controls and KRS patients lacked caspase-8 activity (data not shown). A progressive increase in caspase-8 activity was observed in both groups after 48 hrs of incubation with dRib; however the increase was more evident in PBLs from patients (Fig. 6A and B) than in control (Fig. 6C) PBLs (Table 4). After 48 hrs of culture without dRib, PBLs from KRS patients (Fig. 6D and E) showed a higher percentage of caspase-8 activation than controls (Fig. 6F) (Table 4).

Table 5 shows mean percentages (±S.D.) of PBLs showing caspase-9 activation at 1 and 48 hrs of culture. PBLs from both controls and KRS patients, after 1 hr of incubation with and without dRib, lacked caspase-9 activity (data not shown). In both groups a progressive increase in caspase-9 activity was seen after 48 hrs of incubation with dRib. However, the increase observed in KRS patient PBLs (Fig. 7A and B) was greater than the increase observed in control PBLs (Fig. 7C) (Table 5). Even when cultured without dRib, PBLs from KRS patients (Fig. 7D and E) showed a higher percentage of caspase-9 activation than controls (Fig. 7F) (Table 5).

Discussion

In this study, we have evaluated, for the first time, the presence of apoptosis in cells from two siblings with KRS and their response to the apoptosis inducer dRib, comparing the results with those of a control group. We also had the opportunity to evaluate the apoptotic response of cells from the probands' healthy parents. Our

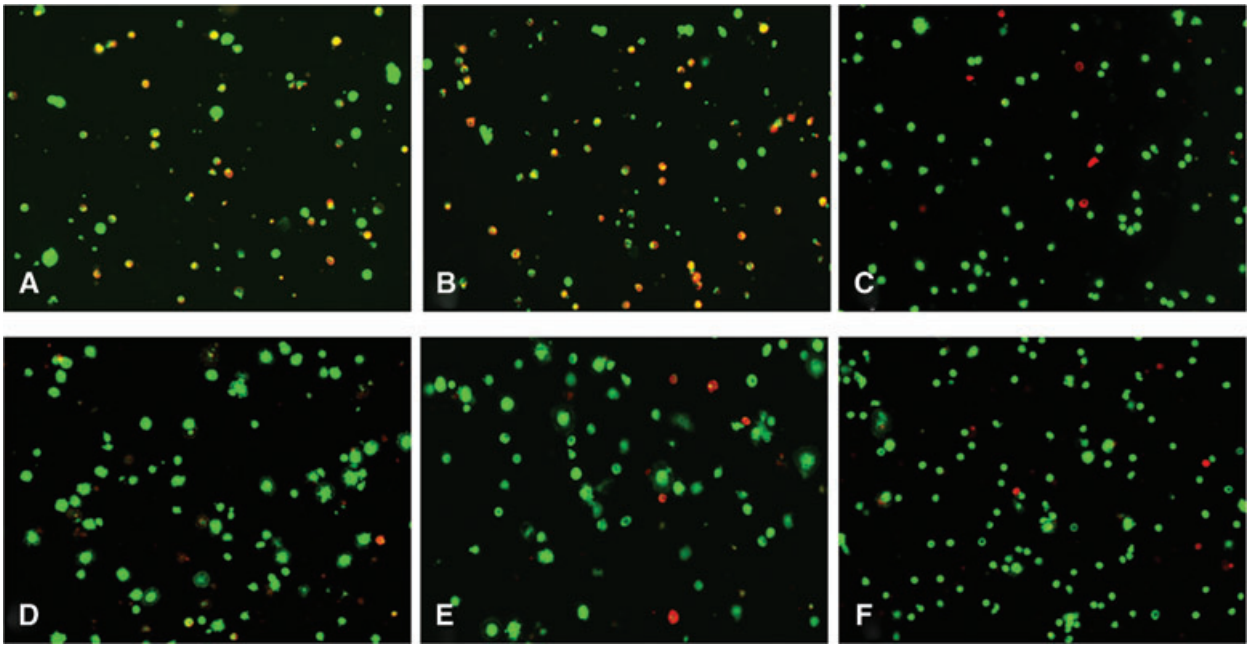

Fig. 4 Apoptosis evaluation with Annexin V (red fluorescence) and 6-DCFA (green fluorescence) staining in PBLs from KRS patients (BC and BA) and a control representing the group, after 48 hrs of incubation with dRib (**A**–**C**) and in standard conditions (**D**–**F**). Magnification 20×.

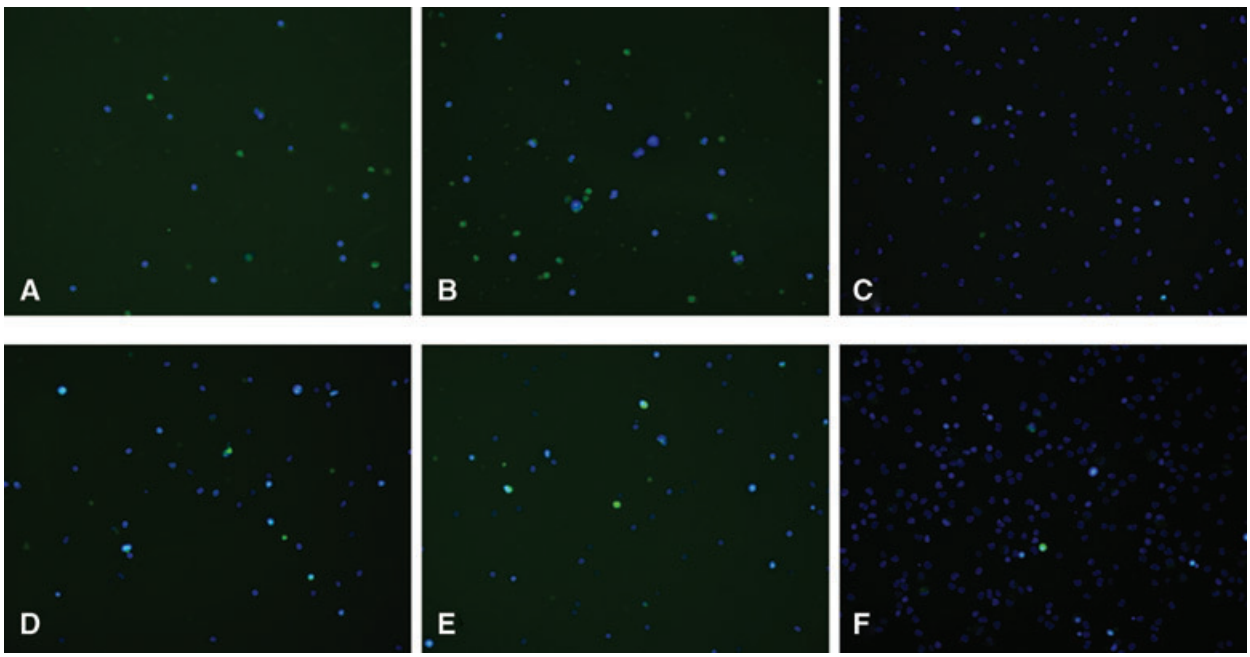

Fig. 5 Analysis of activation of caspase-3 and -7 activation by FLICA FAM-DEVD-FMK (green fluorescence) and simultaneous staining of nuclei with Hoechst 33258 (blue fluorescence) in PBLs from KRS patients (BC and BA) and a control representing the group, after 48 hrs of incubation with dRib (**A**–**C**), and in standard conditions (**D**–**F**). Magnification 20×.

data showed a much higher degree of apoptosis in PBLs from KRS patients than in PBLs from controls both in standard conditions and after exposure to dRib-induced oxidative stress. Moreover, the healthy parents showed an apoptotic pattern similar to that of the KRS patients, with a much higher degree of apoptosis than controls.

Table 3 Mean percentage (±S.D.) of PBLs from KRS patients (BC and BA) and controls (C) showing caspase-3 and -7 activation as analysed by FLICA staining

	BC	BA	C
T1–	0.7 ± 0.1	1.3 ± 0.4	0.5 ± 0.2
T48–	10.9 ± 1.8	12.7 ± 1.5	1.6 ± 0.4
T1+	1.9 ± 0.3	1.8 ± 0.3	0.8 ± 0.2
T48+	38.5 ± 3.6	37.5 ± 3.3	3.3 ± 0.8

Table 4 Mean percentage (±S.D.) of PBLs from KRS patients (BC and BA) and controls (C) showing caspase-8 activation as analysed by FLICA staining

	BC	BA	C
T1–	0.9 ± 0.3	1.1 ± 0.2	1.0 ± 0.3
T48–	5.3 ± 1.1	6.4 ± 1.2	1.6 ± 0.5
T1+	2.2 ± 0.5	2.5 ± 0.7	0.9 ± 0.3
T48+	35.7 ± 3.9	30.1 ± 3.1	2.1 ± 0.7

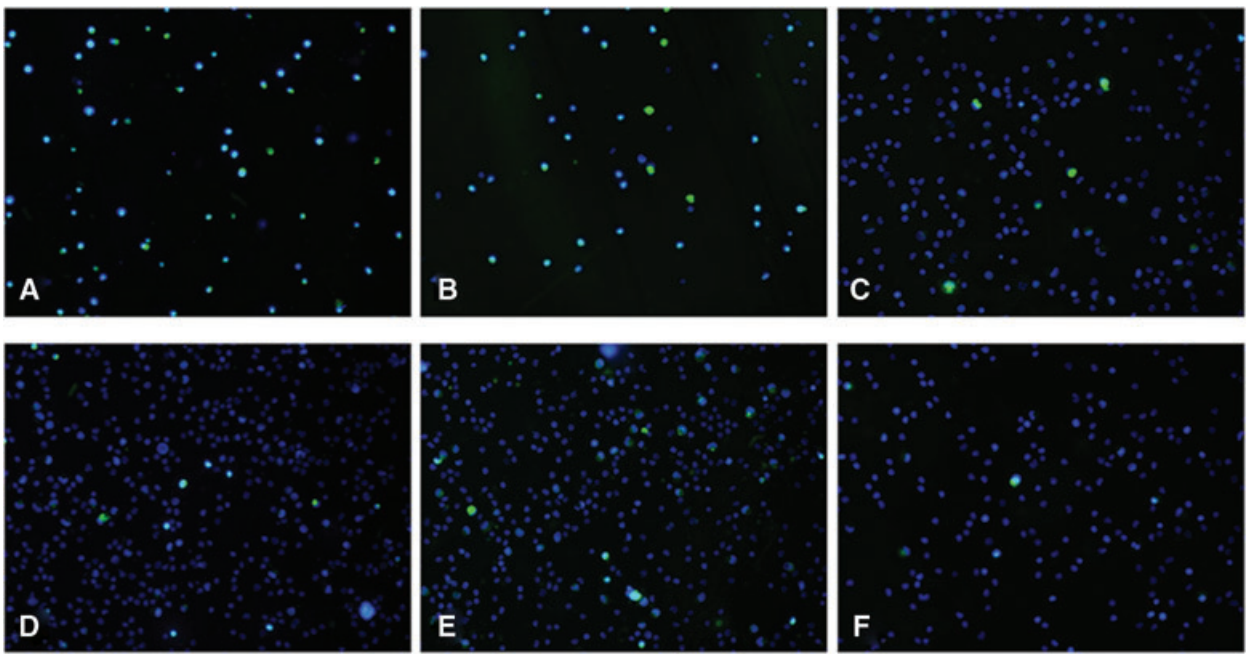

Fig. 6 Evaluation of caspase-8 activation by FLICA FAM-LETD-FMK (green fluorescence) and simultaneous staining of nuclei with Hoechst 33258 (blue fluorescence) in PBLs from KRS patients (BC and BA) and a control representative of the group after 48 hrs of incubation with dRib (**A**–**C**) and in standard conditions (**D**–**F**) after 48 hrs. Magnification 20×.

ATP13A2 is a large lysosomal transmembrane protein member of the P-type ATPase superfamily, characterized by a ten-transmembrane domain topology. ATP13A2 is expressed ubiquitously in the human brain although at different levels, the substantia nigra shows the strongest mRNA expression [18]. P-type ATPases use the energy deriving from ATP hydrolysis to generate ion gradients across membranes [1]. The function and substrate specificity of ATP13A2 protein so far remains unknown, although it is plausible to suggest that it acts as a transporter for an unidentified cation from the cytosol to the lysosomal lumen [1]. The c.G2629A mutation in *ATP13A2* described in the KRS family leads to the p.G877R missense change and causes the replacement of a small non-polar amino acid (glycine) with a large polar one (arginine), in both the catalytic autophosphorylation domain and the nucleotide binding domain of the encoded protein. Therefore, it is conceivable that this mutation interferes with the ATPase and autophosphorylation activity of ATP13A2, negatively affecting the protein's function as a cationic pump [13].

FBXO7 protein is a member of the F-box-containing protein (FBP) family, characterized by a 40-amino acid domain (the F-box) that contains an ubiquitin-like fold in its N-terminal half [19]. Some studies have shown that FBPs serve as molecular scaffolds in the formation of protein complexes, and they have been implicated in a range of processes such as the cell cycle, genome stability, development, synapse formation and circadian rhythms [20]. The function of FBOX7 has not been completely elucidated and it is unclear how the mutation in the *FBXO7* gene leads to Parkinson's disease [19]. It has recently been suggested that

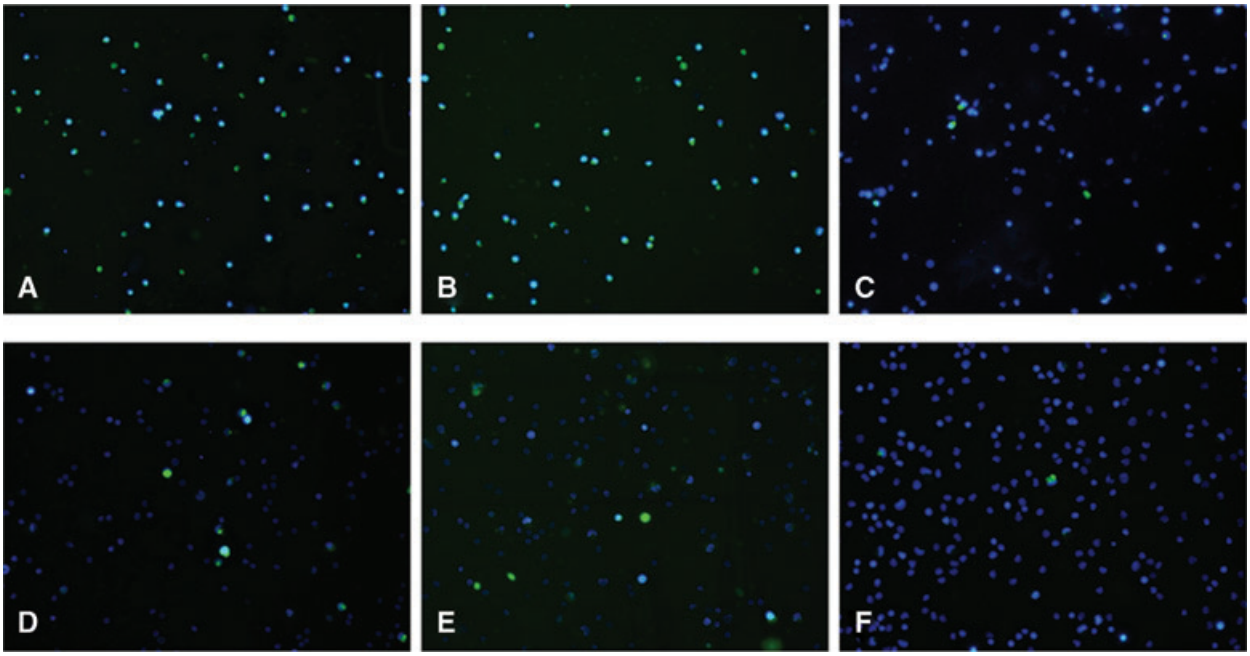

Fig. 7 Analysis of activation of caspase-9 activation by FLICA FAM-LEHD-FMK (green fluorescence) and simultaneous staining of nuclei with Hoechst 33258 (blue fluorescence) in PBLs from KRS patients (BC and BA) and a control representing the group, after 48 hrs of incubation with dRib (**A**–**C**), and in standard conditions (**D**–**F**). Magnification 20×.

Table 5 Mean percentage (±S.D.) of PBLs from KRS patients (BC and BA) and controls (C) showing caspase-9 activation as analysed by FLICA staining

	BC	BA	C
T1–	1.1 ± 0.2	0.9 ± 0.2	0.8 ± 0.2
T48–	10.7 ± 2.9	9.4 ± 1.4	1.2 ± 0.4
T1+	2.5 ± 0.8	2.2 ± 0.1	1.0 ± 0.3
T48+	34.7 ± 4.1	41.7 ± 4.4	4.2 ± 1.1

FBXO7 promotes the ubiquitination of the cIAP1 protein, thus providing important implications concerning the role of FBXO7 in the regulation of this important inhibitor of apoptosis [21].

The first observation emerging from our study was the lack of correlation between the increase in the percentage of apoptotic cells and the presence of the c.C1441T mutation in the *FBXO7* gene. Indeed, both in standard conditions and after the induction of apoptosis, PBLs from the father not carrying the *FBOX7* mutation showed high apoptotic levels, which were comparable to those of the other family members. Our data thus seem to rule out the involvement of FBXO7 in regulating apoptosis in the KRS family analysed.

The altered apoptotic pattern we observed in subjects with the c.G2629A mutation in the *ATP13A2* gene suggests the existence of a possible correlation between the altered regulation of apoptotic mechanisms and the mutated ATP13A2 protein. In particular, we can hypothesize that the mutation in *ATP13A2* may compromise protein function, thus disrupting cell cation balance [4] and generating an altered intracellular milieu that could render cells prone to apoptosis. However, we cannot rule out the existence of some, as yet unknown, interaction between the ATP13A2 protein and key proteins involved in the induction and regulation of apoptotic cell death.

Moreover, the observation that high apoptosis levels were also found in the parents, who were carriers of the *ATP13A2* mutation, shows that heterozygosis may be sufficient to determine an alteration of the apoptotic pathway.

Finally, the fact that apoptosis was deregulated in both the healthy parents and the KRS patients and that the latter displayed such a different disease severity, suggested that the alteration of the apoptotic pathways probably does not have a pathogenetic role in KRS by itself.

In conclusion, we demonstrated the presence of high apoptosis levels in PBLs from subjects carrying the c.G2629A mutation in exon 24 of the *ATP13A2* gene, both in basal culture conditions and after the induction of apoptosis with a stimulus. Nonetheless, our data prompted us to rule out a direct role for apoptosis in the pathogenesis of this form of early-onset Parkinson's disease. On the other hand, the meaning of the elevated levels of apoptosis found in cells from the two KRS patients and their parents still remains to be elucidated and needs further evaluation in other KRS patients.

Acknowledgements

This work was supported by a grant from Ministry of Health and Regione Toscana to A.F.; Contract grant number: AOOGRT/2120/125.002.006.

Author contribution

E.R. and P.F. designed the research study, performed the research, analysed the data and wrote the paper; G.D.M. acquired the data; C.B. and A.F. designed the research study, revised the paper and approved the submitted and final version.

Conflict of interest

The authors confirm that there are no conflicts of interest.

References

1. **Schultheis PJ, Hagen TT, O'Toole KK, *et al.*** Characterization of the P5 subfamily of P-type transport ATPases in mice. *Biochem Biophys Res Commun.* 2004; 323: 731–8.
2. **Kühlbrandt W.** Biology, structure and mechanism of P-type ATPases. *Nat Rev Mol Cell Biol.* 2004; 5: 282–95.
3. **Gitler AD, Chesi A, Geddie ML, *et al.*** Alpha-synuclein is part of a diverse and highly conserved interaction network that includes PARK9 and manganese toxicity. *Nat Genet.* 2009; 41: 308–15.
4. **Schmidt K, Wolfe DM, Stiller B, *et al.*** Cd2+, Mn2+, Ni2+ and Se2+ toxicity to Saccharomyces cerevisiae lacking YPK9p the orthologue of human ATP13A2. *Biochem Biophys Res Commun.* 2009; 383: 198–202.
5. **Najim al-Din AS, Wriekat A, Mubaidin A, *et al.*** Pallido-pyramidal degeneration, supranuclear upgaze paresis and dementia: Kufor–Rakeb syndrome. *Acta Neurol Scand.* 1994; 89: 347–52.
6. **Williams DR, Hadeed A, al-Din AS, *et al.*** Kufor Rakeb disease: autosomal recessive, levodopa-responsive parkinsonism with pyramidal degeneration, supranuclear gaze palsy, and dementia. *Mov Disord.* 2005; 20: 1264–71.
7. **Di Fonzo A, Chien HF, Socal M, *et al.*** ATP13A2 missense mutations in juvenile parkinsonism and young onset Parkinson disease. *Neurology.* 2007; 68: 1557–62.
8. **Deshaies RJ.** SCF and Cullin/Ring H2-based ubiquitin ligases. *Ann Rev Cell Dev Biol.* 1999; 15: 435–67.
9. **Kletsas D, Barbieri D, Stahakos D, *et al.*** The highly reducing sugar 2-deoxy-D-ribose induces apoptosis in human fibroblasts by reduced glutathione depletion and cytoskeletal disruption. *Biochem Biophys Res Commun.* 1998; 243: 416–25.
10. **Battisti C, Formichi P, Tripodi SA, *et al.*** Increased apoptotic response to 2-deoxy-D-ribose in ataxia-telagiectasia. *J Neurol Sci.* 1996; 144: 128–34.
11. **Formichi P, Battisti C, Tripodi SA, *et al.*** Apoptotic response and cell cycle transition in ataxia telangiectasia cells exposed to oxidative stress. *Life Sci.* 2000; 66: 1893–903.
12. **Formichi P, Radi E, Battisti C, *et al.*** Apoptosis in CADASIL: an *in vitro* study of lymphocytes and fibroblasts from a cohort of Italian patients. *J Cell Physiol.* 2009; 219: 494–502.
13. **Santoro L, Breedveld GJ, Manganelli F, *et al.*** Novel ATP13A2 (PARK9) homozygous mutation in a family with marked phenotype variability. *Neurogenetics.* 2011; 12: 33–9.
14. **Boyum A.** Separation of lymphocytes, granulocytes, and monocytes from human blood using iodinated density gradient media. *Methods Enzymol.* 1984; 108: 88–102.
15. **Nicoletti I, Migliorati G, Pagliacci MC, *et al.*** A rapid and simple method for measuring thymocyte apoptosis by propidium iodide staining and flow cytometry. *J Immunol Methods.* 1999; 139: 271–9.
16. **Eastman A.** Assays for DNA fragmentation, endonucleases, and intracellular pH and Ca2+associated with apoptosis. *Methods Cell Biol.* 1995; 46: 41–55.
17. **Lieven CJ, Vrabec JP, Levin LA.** The effects of oxidative stress on mitochondrial transmembrane potential in retinal ganglion cells. *Antioxid Redox Signal.* 2003; 5: 641–6.
18. **Ramirez A, Heimbach A, Gründemann J, *et al.*** Hereditary parkinsonism with dementia is caused by mutations in ATP13A2, encoding a lysosomal type 5 P-type ATPase. *Nat Genet.* 2006; 38: 1184–91.
19. **Luo LZ, Xu Q, Guo JF, *et al.*** FBXO7 gene mutations may be rare in Chinese early-onset Parkinsonism patients. *Neurosci Lett.* 2010; 482: 86–9.
20. **Ho MS, Ou C, Chan YR, *et al.*** The utility F-box for protein destruction. *Cell Mol Life Sci.* 2008; 65: 1977–2000.
21. **Chang YF, Cheng CM, Chang LK, *et al.*** The F-box protein Fbxo7 interacts with human inhibitor of apoptosis protein cIAP1 and promotes cIAP1 ubiquitination. *Biochem Biophys Res Commun.* 2006; 342: 1022–6.